HREM and CIP Characterization of Complex Superstructures in Cu-Co Related Perovskites

Luisa Ruiz-González,[a] Khalid Boulahya,[a] Marina Parras,[a] José Alonso,[b] and José M. González-Calbet*[a]

Keywords: Perovskite phases / Superstructures / Electron diffraction / Electron microscopy

Two compositions in the La-Ba-Cu-Co-O system – $La_2Ba_3Cu_2Co_3O_{13}$ and $La_2Ba_3Cu_3Co_2O_{13}$ – have been synthesized and characterized by means of SAED (Selected Area Electron Diffraction) and HREM (High Resolution Electron Microscopy). The $La_2Ba_3Cu_2Co_3O_{13}$ phase leads to a fivefold perovskite superstructure along the *c* axis, which can be described as formed by the recurrent intergrowth of the two alternating blocks ···*PP*··· and ···PO_hP··· (*P* = pyramid and O_h = octahedron). Pyramidal and octahedral sites are randomly occupied by Cu/Co cations, while La/Ba cations exhibit an ordered distribution. The $La_2Ba_3Cu_3Co_2O_{13}$ composition gives rise to a mixture of phases in which a new phase showing a threefold superstructure due to the sequence ···PO_hP··· coexists with a fivefold superstructure with the same polyhedra sequence (···*PPPO*$_h$*P*···) as the previous one, but a disordered arrangement of lanthanum-barium cations.

Introduction

Extensive research on compositional variations in perovskite ABO_3 related compounds has led to the stabilization of new oxygen-deficient phases $AA'BB'O_{6-x}$ as a consequence of ordered arrangement at the cation and/or oxygen sublattices. Cationic order can be found in both A and B sublattices, and is related to the size and charge differences of each set of cations. Moreover, the coordination tendencies of B cations in the host lattice of oxygen-deficient perovskites can lead to new mixed frameworks with ordered anionic vacancies in which polyhedra-sharing corners can involve octahedral (O_h), square-pyramidal (*P*), tetrahedral (T_h) or square-planar (S_p) units.

For instance, $YBaCuFeO_5$[1] can be described as being built up from the ordered stacking sequence ···*PP*···, whereas octahedra and tetrahedra alternate in an ordered way in $Ca_2(Fe,Al)_2O_5$[2] according to ···$O_hT_hO_hT_h'$··· (T_h' stands for a change of the T_h orientation), and $La_2Ni_2O_5$[3] accommodates square-planar coordination according to the stacking sequence ···O_hS_p···. Other perovskite-related types can be formed when combining the above structural units in a more complex way. For instance, $YBa_2Fe_3O_8$[4] is a threefold perovskite superstructure with iron in octahedral and square-pyramidal coordination according to the sequence ···PO_hP···. Related phases of higher periodicity are obtained if more octahedral layers are added. This is the case for $Ln_2Ba_2Cu_2M_2O_{11}$ (M = Ti, Sn)[5] and $Ln_2Ba_2Ca_2Cu_2Ti_4O_{11}$,[6] which have four- (···$PO_hO_hO_hO_h$···) and sixfold (···$PO_hO_hO_hO_hO_hO_h$···) perovskite superstructures, respectively. On the other hand, ordered intergrowths between perovskite (O_h) and brownmillerite (O_hT_h) units lead to intermediate phases, such as $Ca_2LaFe_3O_8$,[7] $Ca_4Fe_2Ti_2O_{11}$,[8] and $Ca_4YFe_5O_{13}$[9] which stabilize three-, eight-, and tenfold superstructures, exhibiting the ···$O_hO_hT_h$···, ···$O_hO_hO_hT_hO_hO_hO_hT_h'$··· and ···$O_hO_hT_hO_hT_h'O_hO_hT_h'O_hT_h$··· sequences, respectively. In a similar way, $La_4Ni_4O_{11}$[10] stabilizes the ···$O_hO_hO_hS_p$··· sequence, in the La-Ni-O system.

The above compounds are examples of perovskite-related superlattices formed by recurrent intergrowth of two different, but related, structural types. Cases in which intergrowths are non-recurrent, i.e., they do not show long-range ordering along the crystal, have also been described.[11,12] This order-disorder situation can be understood on the basis of the rather complex compositions embracing two or more types of cations for each A and B site of the perovskite sublattice $AA'BB'O_{6-x}$ and the subsequent different oxygen polyhedra. As a consequence of the local nature of such a phenomenon, some of these structures cannot be detected by X-ray powder diffraction (XRD) techniques. This makes the microstructural characterization by means of SAED and HREM essential. Furthermore, the Crystallographic Image Processing (CIP) technique, which is based on the combination of SAED and HREM, has been shown to be useful to gather more reliable structural information, after compensation of the transfer-contrast function (CTF), amplitude and phase correction and symmetry averaging.

[a] Dpto. Química Inorgánica, Facultad de Ciencias Químicas, Universidad Complutense de Madrid, 28040 Madrid, Spain
[b] Instituto de Ciencia de Materiales de Madrid, CSIC, Cantoblanco, 28049 Madrid, Spain

  DOI: 10.1002/ejic.200300136

Among the oxygen-deficient perovskite-related phases, cobaltites and cuprates have been widely studied due to their intriguing electronic and magnetic properties. Since different coordination environments are available for both Cu and Co cations, they are suitable for rather complex pathways of vacancy ordering in non-stoichiometric phases $AA'BB'O_{6-x}$, as recently reported for $LaBaCuCoO_{5.2}$.[13] Its structure (Figure 1) can be described as formed by the recurrent intergrowth of two alternating blocks of $2a_c$, $\cdots PP\cdots$, and $3a_c$, $\cdots PO_hP\cdots$, periodicities (a_c means the basic perovskite unit cell parameter) characteristic of the $YBaCuFeO_5$[1] and $YBa_2Fe_3O_8$[4] structural types, respectively. However, evidence of a cation-ordered arrangement was not found and therefore a random distribution was assumed. In this work, we have tried to induce cation ordering by changing the cationic ratio in both A-A′ and B-B′ perovskite sublattices. In this sense, according to the polyhedra model depicted in Figure 1, corresponding to $LaBaCuCoO_{5.2}$,[13] the La/Ba ratio was kept as 2:3 taking into account the preferred twelve coordination of Ba cations,[14] while different Cu/Co ratios were considered.

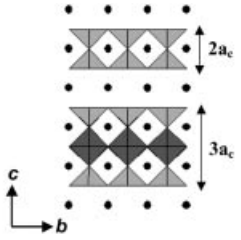

Figure 1. $LaBaCuCoO_{5.2}$ polyhedra model

Results and Discussion

$La_2Ba_3Cu_3Co_2O_y$

The XRD pattern can be indexed on the basis of an orthorhombic unit cell, $a = 0.3948$, $b = 0.3958$, and $c = 1.1683$ nm (Figure 2), characteristic of a threefold perovskite superstructure.[15] However, EDS, SAED, and HREM studies indicate that, besides the threefold superlattice, another phase is apparent. Actually, two kinds of crystals exhibiting a different Cu/Co ratio − $Cu_{0.6}Co_{0.4}$ and $Cu_{0.55}Co_{0.45}$ − have been detected. The corresponding SAED patterns along the $[100]_c$ zone axis are shown in Figure 3 a and b, respectively (subindex c refers to the cubic cell sublattice). In both cases, strong reflections appear, in agreement with the basic perovskite cell. In spite of this, weaker reflections are also present indicating different structural arrangements. In the case of the $Cu_{0.6}Co_{0.4}$ sample, spots at 1/3 and 2/3 appear along c^*, suggesting a threefold perovskite superlattice. Moreover, b^* and $c^*/3$ reciprocal parameters are clearly different, confirming the structural distortion shown in the X-ray diffraction pattern. This is in agreement with the XRD information. When the

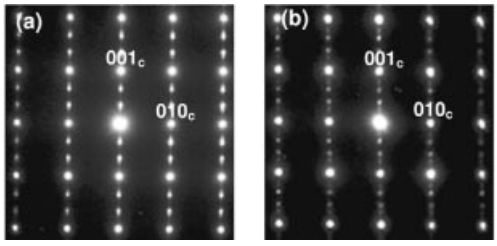

Figure 3. SAED patterns along $[100]_c$ zone axis corresponding to $La_2Ba_3Cu_3Co_2O_y$ sample (a) $Cu_{0.6}Co_{0.4}$ and (b) $Cu_{0.55}Co_{0.45}$ ratio, respectively

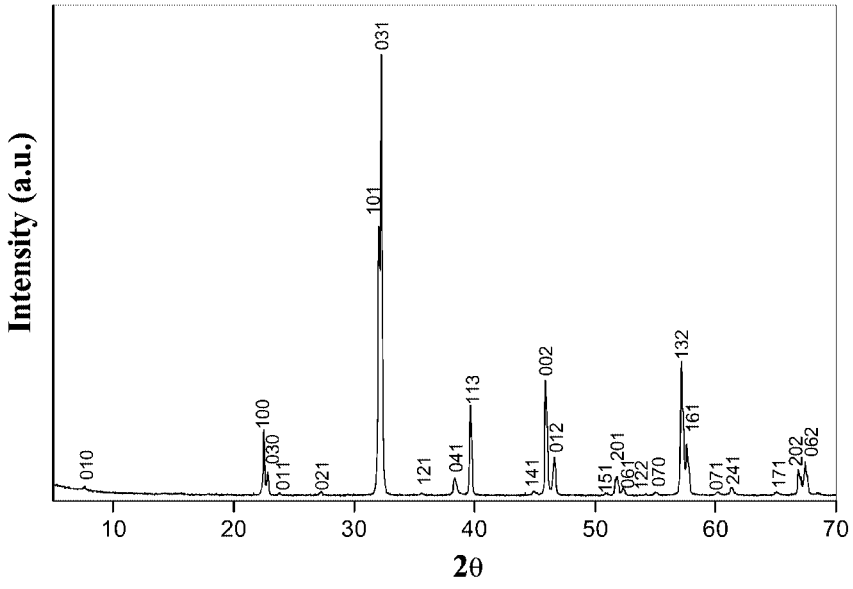

Figure 2. XRD diffraction pattern corresponding to $La_2Ba_3Cu_3Co_2O_y$

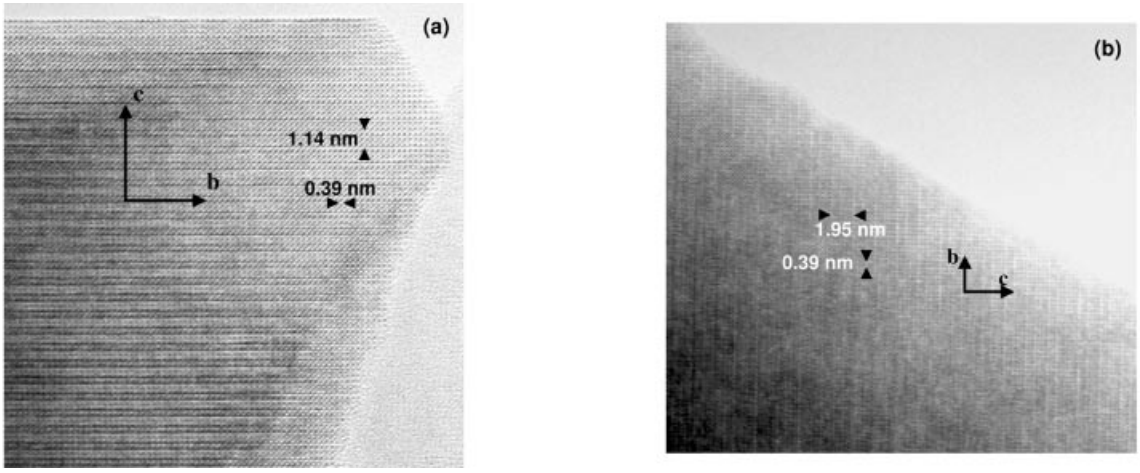

Figure 4. HREM images along $[100]_c$ zone axis corresponding to $La_2Ba_3Cu_3Co_2O_y$ sample (a) $Cu_{0.6}Co_{0.4}$ and (b) $Cu_{0.55}Co_{0.45}$ ratios, respectively

Cu/Co ratio is $Cu_{0.55}Co_{0.45}$, superlattice reflections are placed at 2/5 and 3/5 along c^*, indicating a fivefold perovskite superstructure. The corresponding HREM images (Figure 4, a and b) confirm the above periodicities, i.e, 1.14 and 1.95 nm, along c, for crystals $Cu_{0.6}Co_{0.4}$ and $Cu_{0.55}Co_{0.45}$, respectively.

The threefold order assigned to the $Cu_{0.6}Co_{0.4}$ orthorhombic phase is detected in the XRD pattern. However, the fivefold order previously reported for $LaBaCuCoO_{5.2}$,[13] is not observed. This could be related to the small X-ray powder scattering factor of the oxygen atoms together with the fact that no significant distortions from the basic perovskite sublattice are observed.[13] In this sense, the cubic pattern corresponding to the $Cu_{0.55}Co_{0.45}$ phase (related to $LaBaCuCoO_{5.2}$) must overlap with the one corresponding to $Cu_{0.6}Co_{0.4}$, thus precluding the identification of the former phase by means of XRD.

It is therefore clear that the nominal composition $La_2Ba_3Cu_3Co_2O_y$ leads to a phase mixture, in contrast to $LaBaCuCoO_{5.2}$, which stabilizes a fivefold superlattice built up from the polyhedra sequence $\cdots PO_hPPP\cdots$. The crystal showing Cu/Co = 0.6/0.4 = 1.5 is related to a threefold perovskite superstructure along c. This framework could be obtained by modifying the $2a_c$ periodicity blocks ($\cdots PP\cdots$) in the $LaBaCuCoO_{5.2}$ phase either by suppressing such a block or keeping it while adding one octahedral layer between the two square pyramids. Both pathways would give rise to the stacking sequence $\cdots PO_hP\cdots$, i.e., the basic unit of the $YBa_2Fe_3O_8$ structural type. Threefold periodicity is also found in the well-known lower-oxygen-content $YBa_2Cu_3O_7$[15] superconducting material, in which S_p instead of O_h gives rise to the polyhedra sequence $\cdots PS_pP\cdots$. Furthermore, the oxygen content can be enhanced by Co substitution, i.e., $LnBa_2Cu_{3-x}Co_xO_y$[16] leading, again, to the $\cdots PO_hP\cdots$ unit. Therefore, a similar phase, with Cu/Co = 1.5, seems to be present in this sample. However, since the Cu content in the phase Cu/Co = 0.6/0.4 (1.5) is higher than that corresponding to the fivefold ordered phase (Cu/Co = 0.5/0.5 = 1), we tentatively propose the second mechanism considering that the Cu excess is placed between the two pyramids of the $2a_c$ blocks, leading to the observed $3a_c$ periodicity. On the other hand, crystals exhibiting a higher Co content, i.e., a Cu/Co ratio close to one, Cu/Co = 0.55:0.45 (1.22), show the fivefold superlattice characteristic of $LaBaCuCoO_{5.2}$.[13] This situation could, again, be understood by adding $2a_c$ periodicity blocks, $\cdots PP\cdots$. Accordingly, since the $\cdots PP\cdots$ stacking sequence constitutes the structural unit of $LnBaCo_2O_5$ phases,[17,18] it is feasible to assume that $2a_c$ periodicity blocks are also present in the Cu/Co = 1.2 crystals as they are Co-rich.

Further annealing of this sample does not lead to a single phase. A threefold ordered superlattice is always present and attempts to avoid it were performed by changing the Cu/Co ratio. Since the excess of Cu over Co seems to stabilize a related $YBa_2Cu_3O_7$ phase, the Cu_3Co_2 ratio was reversed, i.e, the nominal $La_2Ba_3Cu_2Co_3O_y$ composition was prepared and characterized.

$La_2Ba_3Cu_2Co_3O_y$

In contrast to $La_2Ba_3Cu_3Co_2O_y$, the X ray diffraction pattern of the title material can be indexed on the basis of a cubic perovskite unit cell (Figure 5), as also reported for $LaBaCuCoO_{5.2}$.[13] EDS analysis, performed on twenty crystals, indicates an average Cu/Co ratio of 0.4:0.6 (0.66), in agreement with the nominal value. However, it is worth pointing out that small areas of some crystals showed a different ratio (Cu/Co = 0.31:0.69 = 0.45), and are therefore Cu-deficient. The oxygen content was estimated to be 13 atoms per unit formula. The compositional data fit with an average composition $La_2Ba_3Cu_2Co_3O_{13}$.

The SAED pattern along $[001]_c$ (Figure 6) is in agreement with the basic cubic perovskite cell, according to the XRD information. Further study of the reciprocal lattice indicates a more complex situation due to the presence of weaker additional reflections (Figure 7). The SAED pattern along $[100]_c$ (Figure 7, a) shows superlattice reflections at 1/5, 2/5, 3/5, and 4/5 of the c^* axis, suggesting a fivefold superstructure. It is worth recalling that this situation is similar

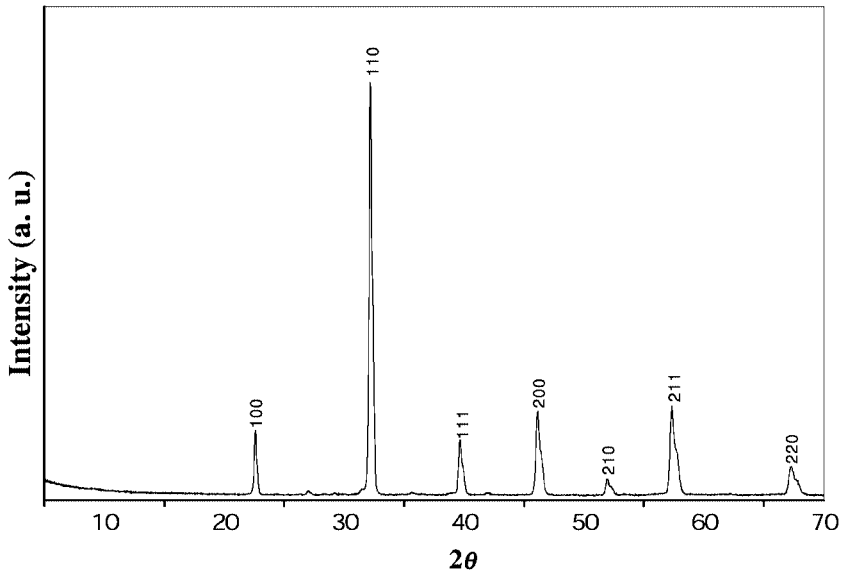

Figure 5. XRD diffraction pattern corresponding to $La_2Ba_3Cu_2Co_3O_y$

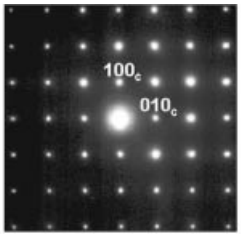

Figure 6. SAED pattern along $[001]_c$ zone axis corresponding to $La_2Ba_3Cu_2Co_3O_y$

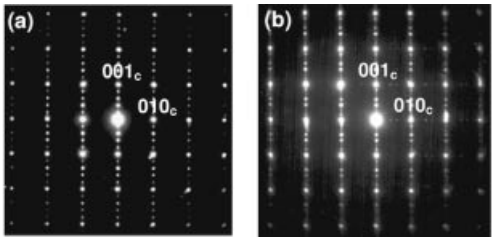

Figure 7. SAED pattern along $[100]_c$ for (a) Cu/Co = 0.4:0.6 and (b) Cu/Co= 0.31:0.69

to that reported for $LaBaCuCoO_{5.2}$,[13] although in this material superstructure streaked spots only appear at 2/5 and 3/5.[13] This difference will be discussed later. Occasionally, another kind of pattern (Figure 7, b), suggesting a sevenfold superlattice, is observed in small areas of the same crystal.

Figure 8 shows an HREM image along the $[100]_c$ zone axis. Two areas, labelled in the image as **1** and **2**, can be observed. Regarding zone **1**, the periodicity along c is 1.95 nm, i.e., related to $5a_c$, in agreement with a fivefold superlattice. FFT (Fourier Transform) performed over this area shows the presence of the corresponding superlattice spots, reinforcing the above suggestion. EDS analysis performed on this area indicates a Cu/Co ratio of 0.4:0.6. A different periodicity is observed at zone **2**, 2.73 nm, i.e., related to $7a_c$, according to the previously suggested sevenfold superstructure. Once again, FFT performed over this area confirms the indicated order. EDS analysis showed a lower Cu/Co ratio (0.31:0.69) in this area.

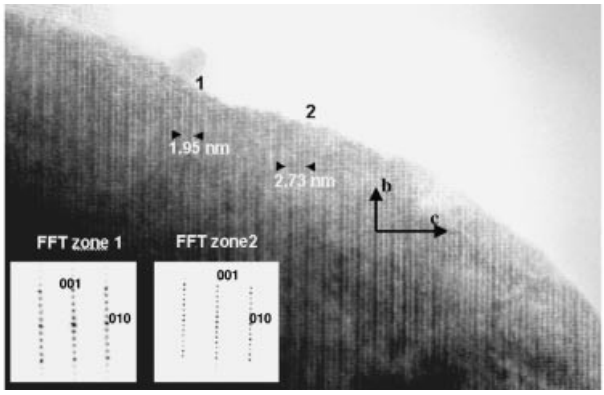

Figure 8. HREM image along $[100]_c$ zone axis corresponding $La_2Ba_3Cu_3Co_2O_y$ sample; two areas, **1** and **2**, exhibiting $5a_c$ and $7a_c$ periodicities, respectively, are labelled

According to these results, it can be concluded that $La_2Ba_3Cu_2Co_3O_{13}$ stabilizes a majority phase, showing a fivefold superlattice, as $LaBaCuCoO_{5.2}$ does. Based on this previous information and also on the structural facts described above, crystallographic image processing (CIP) was performed in order to obtain more reliable structural information. The CIP technique, which combines both SAED and HREM information, allows the gathering of potential maps after performing several corrections and symmetry averaging. In this work, the CRISP program[19] was used for image processing.

Figure 9 (a) corresponds to a thin area of the experimental image along $[100]_c$. Figure 9 (b) is a potential map obtained after the correction of tilt, CTF and the phases and amplitudes of the diffracted beams. After imposing *P2mm*

symmetry, according to the space group *P*4/*mmm* determined by SAED and CBED (Convergent Beam Electron Diffraction), the final potential map depicted in Figure 9 (c) is obtained, in agreement with the fivefold superstructure. Moreover, differences in the black contrast (related to the cation positions) are observed in sites corresponding to La and Ba positions (pointed in Figure 9, c). Such differences are not appreciated at the corresponding B-type positions; in fact, hypothetical order of Cu and Co in these sites could not be detected by this technique, since both cations have close atomic scattering amplitudes for electrons.[20] Although it is not possible to determine the exact oxygen position by CIP, differences in white contrast are observed. It is, in fact, well known that under the optimum defocus conditions the brightest contrast corresponds to the lower potential areas, i.e., oxygen and unoccupied oxygen positions. In this sense, the superstructure must be induced, as also happens with $LaBaCuCoO_{5.2}$, by an ordered arrangement of oxygen vacancies in agreement with the polyhedral model previously mentioned $\cdots PO_hPPP\cdots$, superposed on the potential map. Cobalt and copper must be randomly arranged at the B positions of the basic $AA'BB'O_{6-x}$ perovskite structure, i.e., at the octahedral and pyramidal environments, while La and Ba seem to be ordered along the eight and twelve oxygen coordination sites. According to this, the situation in $La_2Ba_3Cu_2Co_3O_y$ is different to that observed from CIP for $LaBaCuCoO_{5.2}$,[13] whose final potential map does not reveal any cation order arrangement.

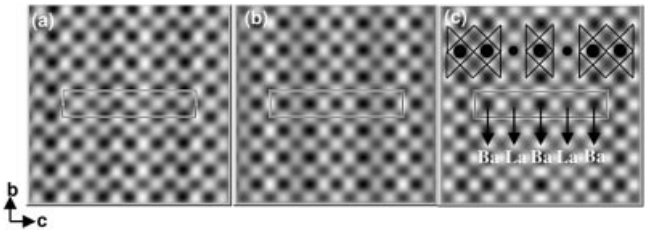

Figure 9. (a) Experimental HREM image corresponding to $La_2Ba_3Cu_3Co_2O_y$; (b) processed image; (c) potential map obtained after applying *pmm* symmetry; the unit cell and structural model are outlined

At this point, it is worth recalling the differences observed between the SAED patterns along $[100]_c$ of the $La_2Ba_3Cu_2Co_3O_{13}$ (Figure 7, a) and $LaBaCuCoO_{5.2}$ (see Figure 2c of ref.[13]) samples, respectively. The first one shows superlattice spots at 1/5, 2/5, 3/5, and 4/5 while the second one only at 2/5 and 3/5, with additional diffuse streaking. On the other hand, since atomic scattering amplitudes for electrons corresponding to La and Ba are different,[20] an ordered distribution of these cations must be detected in the SAED patterns. Accordingly, it seems clear that the observed differences in the above patterns are related to the La/Ba distribution. In order to confirm this assumption, SAED patterns corresponding to the proposed $\cdots PPPO_hP\cdots$ polyhedra sequence with La/Ba ordered and randomly arranged were calculated using the Mac Tempas software package.[21] Table 1 displays the structural parameters used in this calculation for an ordered distribution of La and Ba cations. The corresponding disordered situation has been calculated considering La and Ba distributed at 50% over the three different crystallographic positions.

Table 1. Structural parameters corresponding to $La_2Ba_3Cu_2Co_3O_{13}$ sample; an ordered La/Ba arrangement is considered [space group P4/*mmm* (123), a = 3.9352(3) Å, c = 19.538(2) Å]

Atom	*x*/*a*	*y*/*b*	*z*/*c*	Occ.
Cu/Co1	0	0	0	1
Cu/Co2	0	0	0.203	1
Cu/Co3	0	0	0.395	1
O1	0	0	0.097	1
O2	0	0.5	0.213	1
O3	0	0.5	0.414	1
O4	0	0	0.5	1
O5	0.5	0	0	1
Ba	0.5	0.5	0.1014	1
La	0.5	0.5	0.3010	1
Ba	0.5	0.5	0.5	1

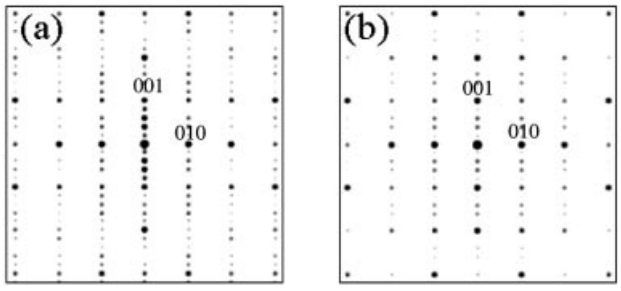

Figure 10. Calculated SAED patterns along $[100]_c$ for $La_2Ba_3Cu_3Co_2O_y$ taking into account the polyhedra sequence $\cdots PO_hPPP\cdots$ and both ordered (a) and random(b) La/Ba distributions

The calculated patterns are shown in Figure 10. When an ordered La/Ba distribution is considered all superlattice reflections are evident (Figure 10, a), while only two extra spots clearly appear when a random distribution is assumed (Figure 10, b). Finally, if La and Ba are ordered in $La_2Ba_3Cu_2Co_3O_{13}$ it could be expected that this fact should also be reflected in the XRD pattern. However, characteristic reflections of the fivefold superstructure do not appear in the experimental pattern (Figure 5). This fact can be explained by taking into account that the atomic scattering factors for X-rays corresponding to La and Ba are equal.[20] In fact, an ordered La/Ba distribution leads to the same X-ray diffraction pattern as for the disordered one.

On the other hand, areas showing sevenfold periodicity can be understood if a $2a_c$ periodicity block ($\cdots PP\cdots$) is added to the $\cdots PO_hPPP\cdots$ sequence, leading to $\cdots PO_hPPPPP\cdots$. At this point, it is worth emphasizing that these areas are Co-rich, so it is plausible to assume that additional $2a_c$ blocks are constituted by pyramidal layers, since this sequence is the basic structural unit of LnBa-

Co_2O_5 compounds.[17,18] Attempts to isolate this sevenfold superstructure are in progress.

This set of results shows that the increase of Co content is accompanied by an increase of the square-pyramidal units in the stacking sequence. In fact, $LnBaCo_2O_{5+\delta}$ [17,18] oxides crystallize in the $\cdots PP\cdots$ stacking sequence whereas $LnBa_2Cu_{3-x}Co_xO_{7\pm\delta}$ [16] shows threefold ordering due to the sequence $\cdots PO_hP\cdots$. When Cu/Co attains a ratio around 1, the $\cdots PPPO_hP\cdots$ polyhedral sequence is stabilized and a fivefold superstructure of the cubic basic cell is observed. This is the case for both $LaBaCuCoO_{13}$[13] and $La_2Ba_3Co_3Cu_2O_{13}$. The difference between both oxides resides in the type of ordering along the A sublattice. While a random situation is obvious in the former, cationic ordering is detected in the latter. The presence of order/disorder in the A sublattice is related to the different oxygen environments involving the A cations in this fivefold superstructure: three sites of twelve coordination and two eight-coordinate sites. This is why only a La/Ba ratio of 2/3 is adequate to obtain an ordered situation.

Experimental Section

Samples of nominal compositions $La_2Ba_3Cu_3Co_2O_y$ and $La_2Ba_3Cu_2Co_3O_y$ were prepared from the apropriate amounts of $BaCO_3$, La_2O_3, Co_3O_4, and CuO. These mixtures were ground in an agate mortar and heated, after carbonate decomposition, at 960 °C for one week with intermediate milling. Cationic compositions were estimated by energy-dispersive X-ray spectroscopy (EDS) using a field-emission electron microscope (FEG) Philips CM200 equipped with an EDAX microanalytical system. Powder X-ray diffraction (XRD) was performed using a Philips X'Pert diffractometer with Cu-K_α radiation. Selected-area electron diffraction (SAED) and high-resolution electron microscopy (HREM) studies were carried out with both JEOL 2000-FX and JEOL 4000-EX electron microscopes. Oxygen content was determined by thermogravimetric analysis using a Cahn D-200 electrobalance equipped with a furnace and a two-channel recorder, allowing simultaneous recording of the weight loss and the reaction temperature. The oxygen content can be determined within $\pm 5\cdot 10^{-3}$ mg for a sample of total mass of about 50 mg.

Acknowledgments

Financial support through research project MAT2001-1440 (Spain) is acknowledged.

[1] L. Er-Rakho, C. Michel, Ph. Lacorre, N. Raveau, *J. Solid State Chem.* **1988**, *73*, 531−535.
[2] E. F. Bertaut, P. Blum, A. Sagnières, *Acta Crystallogr.* **1959**, *12*, 149−159.
[3] M. Crespin, P. Levitz, L. Gatineau, *J. Chem. Soc., Faraday Trans.* **1983**, *79*, 1181−1185.
[4] Q. Huang, P. Karen, V. L. Karen, A. Kjekhus, J. W. Lynn, A. D. Mighell, N. Rosov, A. Santoro, *Phys. Rev. B* **1992**, *45*, 9611−9619.
[5] P. A. Salvador, L. Shen, T. O. Mason, K. B. Greenwood, K. R. Poeppelmeier, *J. Solid State Chem.* **1995**, *119*, 80−89.
[6] K. D. Otzschi, K. R. Poeppelmeier, P. A. Salvador, T. O. Manson, H. Zhang, L. D. Marks, *J. Am. Chem. Soc.* **1996**, *118*, 8951−8952.
[7] J-C. Grenier, F. Ménil, M. Pouchard, P. Hagenmuller, *Mat. Res. Bull.* **1977**, *12*, 79−86.
[8] J. M. González-Calbet, M. Vallet-Regí, *J. Solid State Chem.* **1987**, *68*, 266−271.
[9] Y. Bando, Y. Sekikawa, H. Yamamura, Y. Matsui, *Acta Crystallogr., Sect. A* **1981**, *37*, 723−728.
[10] J. M. González-Calbet, M. J. Sayagués, M. Vallet-Regí, *Solid State Ionics* **1989**, *32/33*, 721−726.
[11] M. Vallet-Regí, J. M. González-Calbet, M. A. Alario-Franco, J. C. Grenier, P. Hagenmuller, *J. Solid State Chem.* **1984**, *55*, 251−261.
[12] J. M. González-Calbet, J. Alonso, M. Vallet-Regí, *J. Solid State Chem.* **1987**, *71*, 331−341.
[13] L. Ruiz-González, K. Boulahya, M. Parras, J. Alonso, J. M. González-Calbet, *Chem. Eur. J.* **2002**, *8*, 5694−5700.
[14] R. D. Shannon, *Acta Crystallogr., Sect. A* **1976**, *32*, 751−767.
[15] J. J. Caponni, C. Chaillout, A. W. Hewat, P. Lajay, P. Marezio, M. Nguyen, N. Raveau, B. Soubeyroux, J. L. Tholence, R. Tournier, *Europhys. Lett.* **1987**, *3*, 1302−1307.
[16] S. Ramesh, N. Y. Vasanthacharya, M. S. Hegde, G. N. Subbanna, H. Rajagopal, A. Sequiera, S. K. Paranjpe, *Physica C* **1995**, *253*, 243−253.
[17] L. Barbey, N. Nguyen, V. Caignaert, M. Hervieu, B. Raveau, *Mat. Res. Bull.* **1992**, *27*, 295−301.
[18] A. Maignan, C. Martin, D. Pelloquin, N. Nguyen, B. Raveau, *J. Solid State Chem.* **1999**, *142*, 247−260.
[19] S. Hovmöller, *Ultramicroscopy* **1992**, *40*, 121−135.
[20] International Tables for Crystallography, *International Union of Crystallography*, **1993**, vol. C.
[21] R. Killas, MacTempas Software 1.7.2, Berkeley Laboratory (UCLA), Berkely, CA.

Received March 12, 2002

